INTERNATIONAL JOURNAL FOR NUMERICAL METHODS IN FLUIDS
Int. J. Numer. Meth. Fluids 2002; **40**:345–351 (DOI: 10.1002/fld.290)

Mapping approach for 3D laminar mixing simulations: application to industrial flows

O. S. Galaktionov*,†, P. D. Anderson, G. W. M. Peters and H. E. H. Meijer

Dutch Polymer Institute, Materials Technology, Eindhoven University of Technology, 5600 MB Eindhoven, The Netherlands

SUMMARY

The computationally efficient *mapping technique* is applied to model laminar mixing in the transport section of the co-rotating twin screw extruder. The technique uses coarse grain values to describe the mixture and exploits temporal and spatial periodicity of the flow. The mapping approach yields adequate description of the concentration fields and residence time distributions. Copyright © 2002 John Wiley & Sons, Ltd.

KEY WORDS: laminar mixing; mapping technique

1. INTRODUCTION

Fluid mixing processes receive significant attention because of their widespread occurrence in nature and especially due to their importance for industrial applications. Mixing of viscous fluids in laminar (low Reynolds number) flows constitutes an important class of mixing phenomena, and is typical for polymer blending, food processing, etc. Numerical simulations of mixing are computationally expensive, especially in 3D, and, therefore, require special methods.

In studying mixing phenomena an accurate determination of the velocity field constitutes, unlike in many hydromechanical problems, only a first, although very important, step. Once the velocity field is known, a variety of techniques based on the tracking of deforming individual fluid volumes [1–3] can be used to study mixing. These direct techniques, however, remain expensive and are only limited to the initial stages of mixing.

Since most spatially bound mixing flows exhibit temporal or spatial periodicity, dynamical system methods like Poincaré maps, periodic points and analysis of their manifolds, etc. are useful, see e.g. [4]. Despite their elegance, these techniques have significant limitations: they

*Correspondence to: O. S. Galaktionov, Dutch Polymer Institute, Materials Technology, Eindhoven University of Technology, 5600 MB Eindhoven, The Netherlands.
†E-mail: o.s.galaktionov@tue.nl

Contract/grant sponsor: Dutch Polymer Institute (DPI); contract/grant number: 161

Received May 2001
Revised October 2001

usually do not provide information on the rate of mixing and characterize only one particular flow. The necessary extensive computations have to be repeated for every minor change to the flow geometry or protocol being introduced. Using these tools to optimize mixing, therefore, is not practical.

The *mapping method* [5] exploits the repetitive nature of most laminar mixing flows and is based on two simple ideas. First, instead of a continuous field of concentration, the mixture is described by locally averaged concentrations in the cells of a properly chosen spatial grid. Second, the flow is presented as a sequence of basic discrete steps, for which a mapping of the concentration distribution during one step is computed. In this paper a brief overview of the basics of mapping technique is given, and its application to the flow in the transport section of the twin screw extruder is described.

2. BASICS OF MAPPING TECHNIQUE

The mapping method was originally proposed by Spencer and Wiley [6] and redefined in a computationally efficient way by Kruijt *et al.* [5]. The flow domain Ω is subdivided into n non-overlapping sub-domains Ω_i with boundaries Γ_i (*not* related to the mesh on which the velocity field is computed). The boundaries of the sub-domains are tracked from $t = t_0$ to $t = t_0 + \Delta t$ using an adaptive front tracking technique [1]. The coefficient Φ_{ij} of the mapping matrix $\mathbf{\Phi}$ is defined as the fraction of the reference (as at $t = t_0$) sub-domain Ω_i, occupied by the deformed sub-domain Ω_j at time $t = t_0 + \Delta t$:

$$\Phi_{ij} = \int_{\Omega_j|_{t=t_0+\Delta t} \cap \Omega_i|_{t=t_0}} \mathrm{d}V \Bigg/ \int_{\Omega_i|_{t=t_0}} \mathrm{d}V \tag{1}$$

Computation of the intersection volume, illustrated by Figure 1, involves an appropriate refinement of the surface grid, describing the deformed cell and the subsequent collapse of all parts of the surface that lie outside the sub-domain with which the intersection is being computed. The matrix $\mathbf{\Phi}$ is essentially sparse due to the fact that, given the relatively small

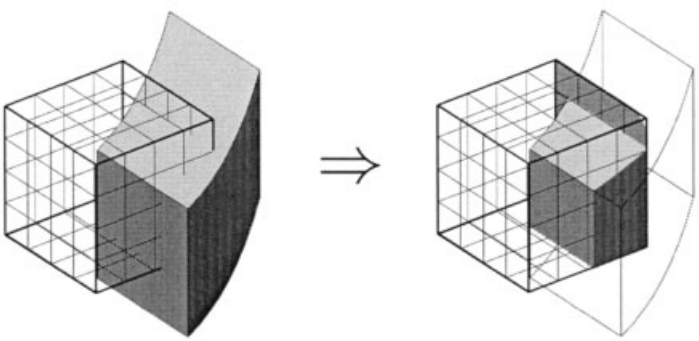

Figure 1. Computation of the elements of the mapping matrix $\mathbf{\Phi}$: determining the volume of the intersection of the deformed cell with initial cells.

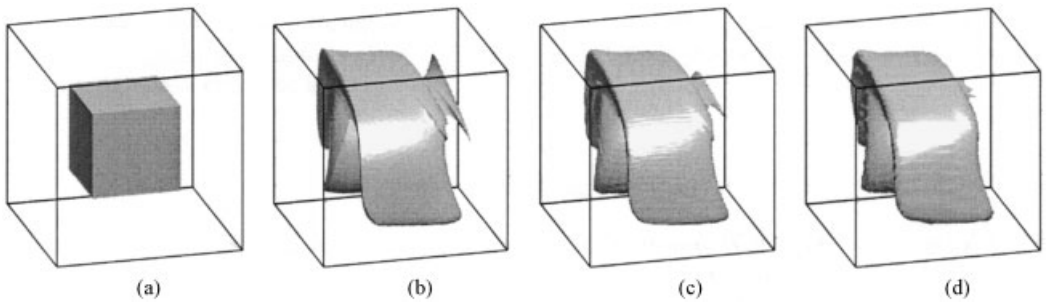

Figure 2. Comparison of front tracking and mapping results in a 3D cavity flow. The flow is generated by four consecutive displacements of front and back wall in X and Z directions: (a) initial test volume; (b) results of adaptive front tracking; (c) interface shape recovered from the mapping results on $100 \times 100 \times 100$ grid, (d) mapping on coarser $(50 \times 50 \times 50)$ grid.

time step Δt, the fluid from one sub-domain is transported to a limited number of resulting sub-domains.

Quantities being mapped should be additive and should not change the flow field. Since the mapping method assumes an uniform distribution of the mapped quantity within each sub-domain, contributions from different donor sub-domains are averaged. This averaging on every step leads to a systematic error, that can be considered as 'numerical diffusion' (since it blurs the sharp boundaries). It sets the limits on the acceptable maximum size of sub-domains. The accuracy of the mapping technique is addressed in more detail in References [7, 8].

The concentration (of marker fluid) distribution is described by a vector $\mathbf{C}$, its components C_i are the locally averaged concentrations in the sub-domains Ω_i. If the distribution at $t_0 = 0$ is described by the vector $\mathbf{C}^0$, the concentration after time Δt is computed as $\mathbf{C}^1 = \mathbf{\Phi C}^0$. The concentration after n similar steps is $\mathbf{C}^n = \mathbf{\Phi}^n \mathbf{C}^0$. The idea of the mapping method was originally formulated by Spencer and Wiley [6], who proposed to analyse the mixing behaviour by studying $\mathbf{\Phi}^n$. However, this is not suitable for high spatial resolutions, since the matrix $\mathbf{\Phi}^n$ will not be sparse and, thus, becomes prohibitively large. The concentration vector $\mathbf{C}^n$ is computed instead in a sequence $\mathbf{C}^{i+1} = \mathbf{\Phi C}^i$. The properties of the mapping matrix itself (especially the meaning of its eigenvalues and eigenvectors) are addressed in Reference [7], using a simple two-dimensional prototype flow.

The mapping approach was tested for 2D and 3D prototype mixing flows and proved to be fast and useful for the optimization of the mixing flow protocols. The technique was also validated by comparing its results to the results produced by explicit front tracking. Figure 2 shows such a comparison for a prototype flows in a cubic cavity [9]: mapping on different grids is compared to adaptive front tracking.

3. RESULTS: TRANSPORT SECTION OF TWIN SCREW EXTRUDER

The technique is here applied to the Stokes flow of a Newtonian fluid in a real industrial-type mixing device: the transport section of a co-rotating twin screw extruder (TSE) [10]. Devices of this type are widely used for melting, pumping and blending of polymers. Four

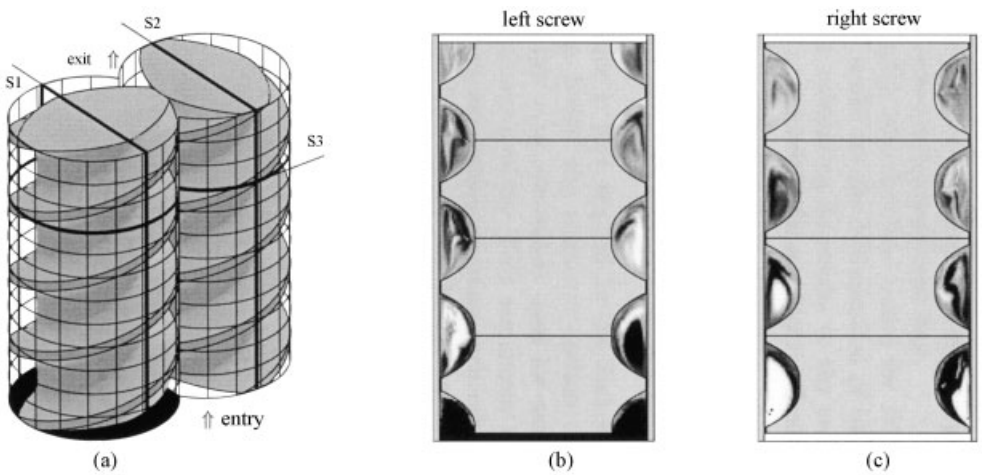

Figure 3. (a) Transport section of the twin screw extruder. Concentration patterns in the cross-sections: (b) **S1** (left screw) and (c) **S2** (right screw).

conveying elements of the TSE are shown in Figure 3(a). Screws are tightly intermeshing and have a self-wiping shape, scraping each others surface during rotation. Both screws rotate counter-clockwise viewed from the bottom in the direction of the flow.

A fictitious domain technique [11] implemented in the finite element package SEPRAN [12] was used to compute the velocity field inside this mixing device. An unstructured mesh, consisting of tetrahedra was used to compute the velocity field, using the $P_1^+P_1$ MINI elements. The helical shape of the screws allows the use of only a single velocity field, accounting for the angle of a screw rotation in time by means of an appropriate axial shift of the reference co-ordinate system.

The computed mapping matrix describes the transport of the material contained originally in one mixing element (spatial period of the mixer—see Figure 3(a)) during a 90° turn of the screws. The grid of the recipient cells has to cover two periods of the mixer: the same as the initial cells plus one mixing element downstream, since the material is being transported along the extruder (thus, partially moving to the next mixing element). The matrix is essentially sparse: only $\approx 13 \times 10^6$ of the totally $\approx 1.56 \times 10^{12}$ elements are non-zeroes (the grid covering one screw element has a resolution 184×100 across the barrel and 48 cells along it). The matrix describing the transport in the whole transport section of the extruder of arbitrary length contains identical blocks on the diagonal and it is never assembled. For more complex screw configurations including other types of the mixing elements, various other building blocks will be required.

Special algorithm for sparse matrix storage (column-oriented but not *physically* ordered) facilitates the efficient parallelization with a dynamical workload distribution: matrix entries can be filled in an arbitrary order. Note, that after the computation of the mapping matrix is accomplished, it can be converted to a more conventional column-oriented ordered storage, which saves up to 25% of memory and makes matrix–vector multiplication on average 30% faster. Computations of the mapping matrix required approximately one year of CPU time

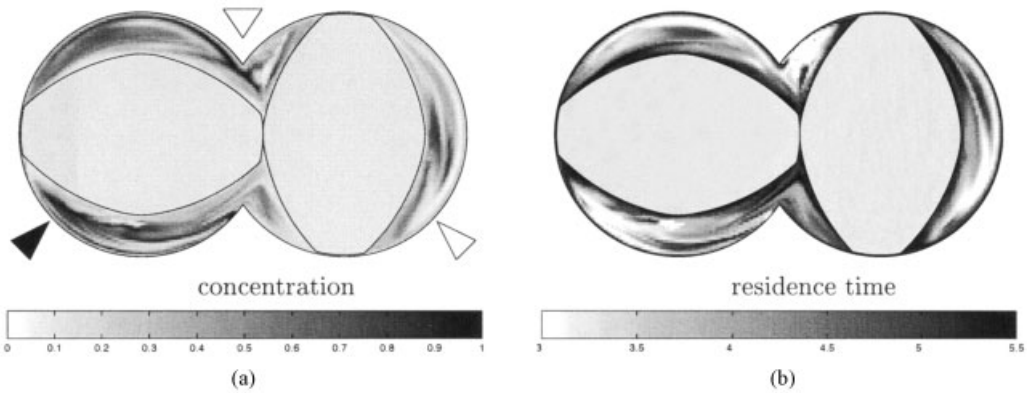

Figure 4. Concentration and residence time distribution in the cross-section **S3** (see Figure 3(a)).

(note, that this is *cumulative* time, parallelization makes it much more affordable). In contrast, the mapping itself is fast and requires less than 3 s per mixing element on a single CPU, and it is this property which makes the method attractive for studying mixing.

Figure 3(b) and 3(c) shows the example of the mapping results: filling of an extruder by two differently coloured fluids. Black fluid enters in the left channel. Four mixing elements are shown. Incoming fluid reaches the exit after approximately 3.5 screw turns, while the concentration pattern nearly stabilizes after 6 rotations. In general, the distinction is made between incoming material and fluid pre-filling the extruder.

Figure 4(a) shows the concentration patterns formed in the cross-section **S3** in the third mixing element. The mapping technique also allows to calculate the residence time distribution. The material entering the mixer has by definition zero residence time. The residence time is carried with material (mapped the same way as concentration) and incremented on every time step. The results of these simulations are shown in Figure 4(b), where the residence time is measured in screw rotations. It is clear that the residence time distribution is rather wide with 'old' material found mainly at the surface of the screws: they are wiped by each other less efficiently, since the contact between screws is only local, while long contact line is formed with the barrel. In addition each spot on the screw is scraped once per full rotation, while the barel in the current configuration is being scraped twice.

Residence time distribution is an important characteristic of the dynamical mixing device. The requirements to it are two-fold: the distribution should be wide enough to 'erase' unavoidable input irregularities and sufficiently narrow to avoid stagnation. The latter requirement is important because the materials being mixed (molten polymers) are often subject to thermal degradation (chemical reactions, etc.).

The effect of the rather wide residence time distribution becomes clear in the simulation of the *pulse feed* test. 'Pulse feed' is a conventional experimental way to measure the residence time distribution. A tracer (often TiO_2) is added during a short period to the material that enters the extruder. At the exit the samples are collected and the amount of tracer measured. Figure 5 shows the results of the simulation of the pulse feed test using the mapping technique. Tracer material is injected during one rotation of the screws. Each mapping step the amount

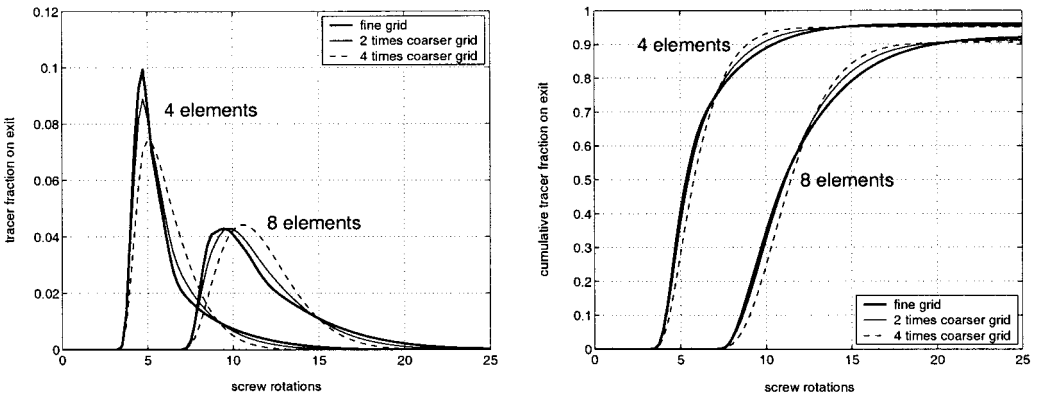

Figure 5. Results of the pulse-feed simulation of four-element and eight-element transport section of extruder: instantaneous and cumulative output (right).

of tracer that exits the fourth element of mixer is determined. After four elements a mismatch between the amount of incoming and exiting tracer due to numerical errors amounts to 4% of the total injected amount. The tracer output reaches its maximum after 4.75 screw turns, and 66% of the total output reaches the exit during the first 6.5 rotations, while it takes 19 screw turns to get 99.5% of the exiting material out (see Figure 5(b)). It is clearly illustrated by Figure 5(a) that after twice longer transport section the tracer output has broader maximum, indicating a wider residence time distribution. The pulse feed test simulations were performed on mapping grids of different size, the results showing a good convergence (see Figure 5).

4. CONCLUSIONS AND FUTURE WORK

The mapping approach allows a fast and efficient simulation of distributive mixing, even in complex industrial flow configurations. Although large number of computations has to be performed in advance to obtain the mapping matrices, they are easily parallelized. Mapping simulations, in contrast, are performed within a few minutes on a single CPU.

The flow in the transport section of the twin screw extruder was studied. The mapping technique makes it possible to examine the process of filling the extruder and to resolve the forming concentration patterns. It also provides an easy way to assess such a practically important characteristic as a residence time distribution. The simulations clearly show the zones where the most ‘old’ material is likely to be found.

The future work is to use the mapping approach for optimization of the extruder design. Mapping matrices for different types of screw elements, including various kneading and pressure-building elements, have to be computed. To reduce the computational costs involved, a smoother solution for the velocity field should be obtained using higher-order finite elements. To increase the efficiency, the sub-domain grid has to be adapted to the extruder geometry. Figure 6 schematically shows the difference between the general rectangular grid and the grid tailored for the extruder geometry. Another important direction is the adaptation of the 3D

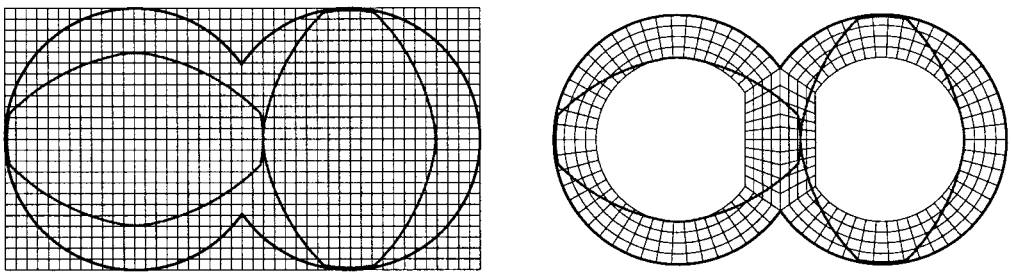

Figure 6. Comparison of the transversal slices of regular rectangular and 'double-cylindrical' coarse grids.

technique to incorporate the statistical description of the microstructure [7, 8] on the sub-grid scale.

REFERENCES

1. Galaktionov OS, Anderson PD, Peters GWM, van de Vosse FN. An adaptive front tracking technique for three-dimensional transient flows. *International Journal for Numerical Methods in Fluids* 2000; **32**(2):201–218.
2. Rudman M. Volume-tracking methods for interfacial flow calculations. *International Journal of Heat & Fluid Flow* 1997; **24**:671–691.
3. Unverdi SO, Tryggvason G. Computations of multi-fluid flow. *Physics of Fluids D* 1992; **60**:70–83.
4. Ottino, JM. *The Kinematics of Mixing*: *Stretching*, *Chaos and Transport*. Cambridge University Press: Cambridge, 1989.
5. Kruijt, PGM, Galaktionov OS, Anderson PD, Peters GWM, Meijer HEH. Analyzing fluid mixing in periodic flows by distribution matrices. *AIChE Journal* 2001; **47**:1005–1015.
6. Spencer, RS, Wiley RH. The mixing of very viscous liquids. *Journal of Colloid Science* 1951; **6**:133–145.
7. Anderson PD, Galaktionov OS, Peters GWM, Meijer HEH, Tucker III CL. Material stretching in laminar mixing flows: extended mapping technique applied to journal bearing flow. *International Journal for Numerical Methods in Fluids* 2002; **40**:189–196.
8. Galaktionov OS, Anderson PD, Peters GWM, Tucker III CL. A global, multi-scale simulation of laminar fluid mixing: the extended mapping method. *International Journal of Multiphase Flows* 2002; **28**(3):497–523.
9. Galaktionov OS, Anderson PD, Kruijt PGM, Peters GWM, Meijer HEH. A mapping approach for 3D distributive mixing analysis. *Computers & Fluids* 2001; **30**(3):271–289.
10. Kruijt, PGM. Analysis and optimization of laminar mixing (design, development and application of the mapping method). *Ph.D. Thesis*, Eindhoven University of Technology: The Netherlands, 2000. http://www.mate.tue.nl.
11. Glowinski R, Pan T-W, Periaux J. A fictitious domain method for external incompressible viscous flow modeled by Navier–Stokes equations. *Computational Methods in Applied Mechanics and Engineering* 1994; **112**:133–148.
12. Segal A. SEPRAN user manual, standard problems and programmers guide. *Ingenieursburo SEPRA*, Leidschendam, 1984.

